Natural Resources for Human Health
eISSN: 2583-1194

Original Research

Received: 11 August 2026
Revised: 14 October 2026
Accepted: 27 October 2026

Natural Resources for Human Health 2026, Vol. 6 (6): 570–595

KEYWORDS:
Solenostemma argel; polarity-guided fractionation; phenolic compounds; antioxidant activity; α-glucosidase inhibition; antimicrobial activity.

Polarity-Guided Fractionation Separates Antioxidant from α-Glucosidase Inhibitory Activities in Solenostemma argel from Central Sahara, Algeria

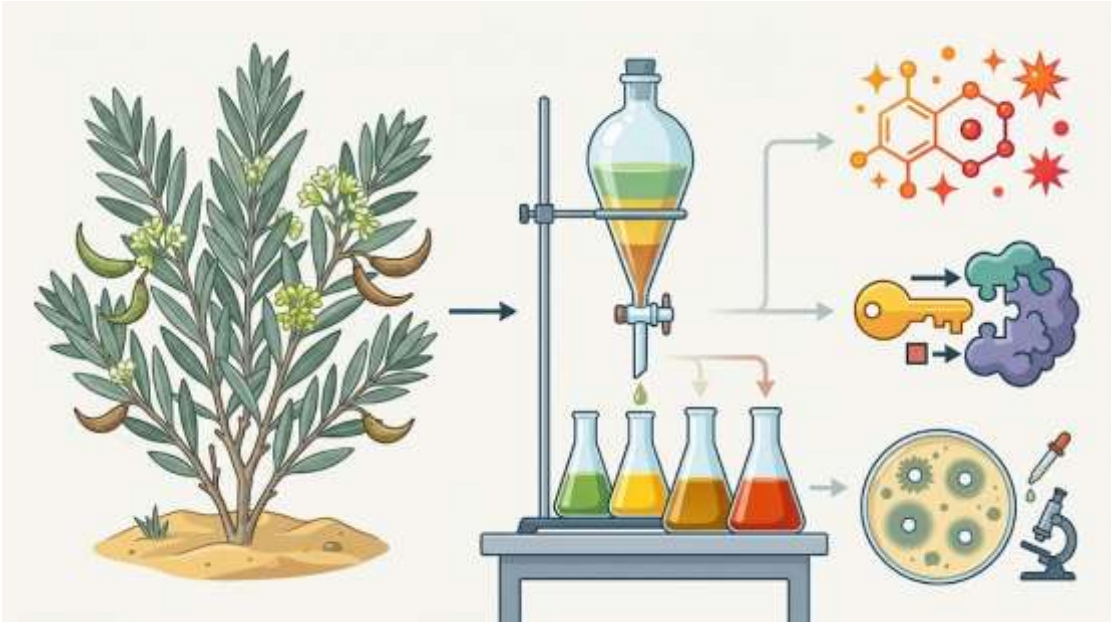
Lamia Aliouche[1], Hanène Zater[1,2]*, Souad Hamimed[2], Sara Mokhtari[3,4]

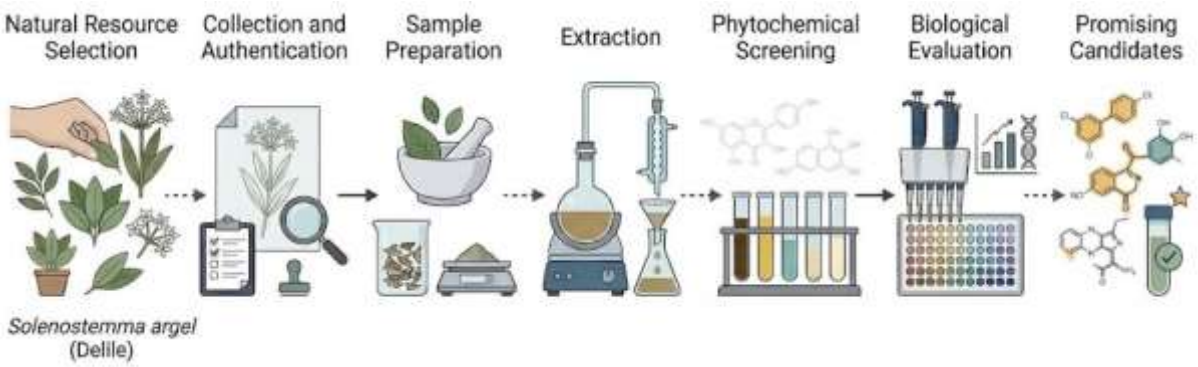
[1]Research Unit for the Valorization of Natural Resources, Bioactive Molecules, and Physicochemical and Biological Analyses (VARENBIOMOL), Department of Chemistry, Faculty of Exact Sciences, University of Constantine 1 Frères Mentouri, Chaabet Ersas Campus, Aïn El Bey Road, 25000 Constantine, Algeria.
[2]Department of Matter Sciences, Faculty of Exact Sciences and Natural and Life Sciences, Larbi Ben M'hidi University of Oum El Bouaghi, Constantine Road, P.O. Box 358, 04000 Oum El Bouaghi, Algeria.
[3]Laboratory of Physiology of Nutrition and Food Safety, Department of Biology, Faculty of Natural and Life Sciences, University of Oran 1 Ahmed Ben Bella, B.P. 1524, El M'Naouer, 31000 Oran, Algeria.
[4]Faculty of Nature and Life Sciences, Department of Biology, Ibn Khaldoun University, P.O. Box 78, Zaaroura, 14000 Tiaret, Algeria.
*Corresponding author: zater.hanene@gmail.com; zater.hanene@univ-oeb.dz

ABSTRACT: Solenostemma argel (Delile) Hayne (Apocynaceae) is a Saharan shrub used in traditional medicine to treat digestive and metabolic disorders, yet data on Algerian material, particularly at the fraction level, remain scarce. We studied the aerial parts collected in Djanet (Central Sahara, Algeria) and compared four fractions of increasing polarity (petroleum ether, chloroform, ethyl acetate, and n-butanol) obtained from a 70% methanolic crude extract. Proximate composition and total phenolic and flavonoid contents were determined, and biological activities were evaluated by three antioxidant assays (DPPH, ABTS$^{\bullet+}$, and phenanthroline), α-glucosidase inhibition, disc diffusion, and radial mycelial growth. The plant material exhibited a moisture content of 10.39 ± 0.31% and a dry matter content of 89.61 ± 0.31%. The dry matter consisted of 3.99 ± 0.21% total ash and 85.62 ± 0.23% organic matter, while the crude fat content was 1.64 ± 0.06%.The n-BuOH and EtOAc fractions had the highest phenolic (339.33 ± 2.85 and 324.46 ± 1.99 µg GAE/mg, respectively) and flavonoid (233.47 ± 1.87 and 218.06 ± 1.95 µg QE/mg, respectively) contents. The n-BuOH fraction was the most active in the DPPH and ABTS assays (IC_{50} = 76,70 ±3.41 and 53.45 ± 1.07µg/mL, respectively), followed by EtOAc. In contrast, within the tested range (6.25–400 µg/mL), only the $CHCl_3$ extract inhibited α-glucosidase (IC50 = 164 ± 0.50 µg/mL), a lower value than that of acarbose (275.43±1.59 µg/mL). Against three strains tested, the EtOAc fraction was the most effective against Escherichia coli and Fusarium oxysporum f. sp. lycopersici, followed by the $CHCl_3$ fraction. Polarity-guided fractionation thus separated radical-scavenging activity from α-glucosidase inhibition, suggesting that different constituents are involved. These in vitro findings offer only partial support for the traditional metabolic use of the plant, and targeted phytochemical

Natural Resources for Human Health
eISSN: 2583-1194

profiling is now needed to isolate and identify the active compounds.





Highlights

- Polarity-guided fractionation of *Solenostemma argel* from the Central Sahara
- *n*-BuOH and EtOAc fractions had the highest phenolic and flavonoid contents
- *n*-BuOH fraction was the most active in the DPPH and ABTS assays
- Only the $CHCl_3$ fraction inhibited α-glucosidase (IC_{50} = 164 ± 0.50 µg/mL),
- EtOAc fraction was the most active against *E. coli* and *F. oxysporum*

1. INTRODUCTION

Plants of the Central Sahara grow under intense heat, drought and irradiation, and are regarded as a promising source of bioactive secondary metabolites (Ksouri et al., 2012). *Solenostemma argel* (Delile) Hayne, a perennial shrub of North African arid zones, is used in folk medicine, notably for digestive disorders and as a febrifuge (Benmaarouf et al., 2020). In the Central Sahara, particularly in the Tassilin'Ajjer region, local pharmacopoeia heavily relies on this species for its broad therapeutic spectrum (Hammiche & Maiza, 2006). Early chemical work on this species concentrated on steroidal constituents. Fifteen 14,15-secopregnane glycosides (argelosides A to J) and nine 15-ketopregnane glycosides (stemmosides C to K) were isolated from pericarps, seeds and leaves and tested for antiproliferative effects in Kaposi's sarcoma cells (Perrone et al., 2008);

argelosides were also described earlier (Plaza et al., 2005). Flavonoids and phenolics have received comparatively less attention. Kaempferol glycosides from the stem were linked to antibacterial and antioxidant activity (Shafek & Michael, 2012), and an acetone extract of Algerian leaves was characterised by UHPLC and MS and tested for antioxidant, anti-inflammatory and antinociceptive effects (Benmaarouf et al., 2020). Metabolic activity has also been investigated. In a comparison of five medicinal plants, *S. argel* was the most active in inhibiting pancreatic lipase, alpha-amylase and alpha-glucosidase and showed antioxidant capacity in DPPH and reducing power assays; the methylene chloride and n-butanol extracts were then examined further (El-Shiekh et al., 2019). In rats, an aqueous extract of leaves and bark lowered blood glucose and alpha-amylase activity (Taha&Bakhit, 2014).

Sequential partition across solvents of rising polarity and bioactivity guided evaluations have proven highly effective in our previous investigations of Algerian flora to relate extract chemistry to a wide range of biological endpoints. This comprehensive approach has been successfully applied by our research group to map phenolic and flavonoid profiles alongside their antioxidant, antidiabetic, cytotoxic, and antimicrobial activities in various local species, including *Serratula cichoracea* (Aliouche et al., 2018; Aliouche et al., 2022), *Achillea ligustica* (Boudjerda et al., 2008), and *Anacyclus pyrethrum* (Hamimed et al., 2018). A similar strategy has also been used to evaluate the antioxidant and anticholinesterase potential of traditional Algerian cereal-based products, including unfermented and fermented wheat as well as couscous prepared from fermented wheat "El Hammoum" (Mokhtari et al., 2016; Mokhtari et al., 2020a; Mokhtari et al., 2020b). Furthermore, extensive chemical and biological profiling has been conducted on several *Centaurea* species from Algeria, yielding potent antimicrobial agents, novel sesquiterpene lactones, and essential oils with notable antibacterial properties (López-Rodríguez et al., 2009; Zater et al., 2014; Zater et al., 2016; Zater et al., 2019a; Zater et al., 2019b; Zater et al., 2021). Although these data concern different genera and families, they serve here as a robust methodological precedent for the systematic evaluation of Saharan botanical resources.

Despite the established therapeutic potential of *S. argel*, a critical research gap remains. Previous biological evaluations have predominantly focused on crude extracts or *in vivo* models without detailed phytochemical correlation, and the plant material was sourced from vastly different geographical regions. The specific ecotype growing in the hyper-arid environment of Tassilin'Ajjer in Djanet, which likely expresses a distinct secondary metabolite profile due to extreme abiotic stress, has never been systematically investigated through polarity guidedextractation. To address this gap and building upon our established methodology, this study aimed to first establish the proximate composition of the aerial parts from this specific Saharan region; second, map the phenolic and flavonoid contents across the three distinct extracts ($CHCl_3$, AcOEt, and *n*-BuOH); and third, directly correlate extract polarity to a comprehensive panel of biological targets encompassing antioxidant capacity, alpha-amylase inhibitionand antimicrobial effects.

2. MATERIALS AND METHODS

2.1. Plant material, collection site and taxonomic identification

Aerial parts of *Solenostemma argel* (Delile) Hayne (also cited as *S. argel*; Figure 1) were collected in May 2023 at Djanet, in the Tassilin'Ajjer region of the Central Sahara, southeastern Algeria (24°33'18" N, 9°29'06" E; Figure 2). The site lies at about 1,050 m above sea level, on a rocky sandstone plateau cut by sandy wadi beds, and supports sparse xerophytic vegetation adapted to arid conditions (Ozenda, 2004). Djanet has a hot desert climate (Köppen-Geiger type BWh); climate normals for 1991 to 2020 give a mean annual temperature of 23.2 °C and a mean annual precipitation of about 16.7 mm (Peel et al., 2007; World Meteorological Organization, 2021).

The plant was identified by Prof. Khellaf Rebbas (University of M'sila, Algeria) from diagnostic morphological characters, with reference to Nouvelle flore de l'Algérie et des regions désertiques méridionales (Quézel and Santa, 1962-1963). The accepted name was checked in Plants of the World Online (POWO, 2026). A voucher specimen (N°. KR0181) was deposited in the personal herbarium of Prof. Rebbas at the University of M'sila. After collection, the aerial parts were dried in the shade at ambient temperature for one week and ground to a fine powder with a particle size of approximately 0.5 mm (equivalent to a 35 mesh sieve) before analysis.

Natural Resources for Human Health
eISSN: 2583-1194



Figure 1: Aerial parts of *Solenostemma argel* (Delile) Hayne used in this study (voucher KR0181), collected at Djanet in May 2023.

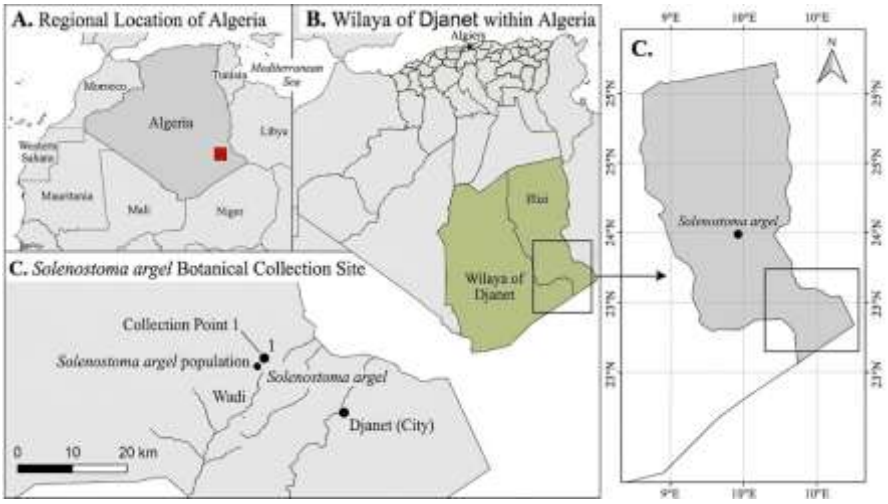


Figure 2: Geographic location and botanical collection site of *Solenostemma argel* in the Wilaya of Djanet, southeastern Algeria (Exact GPS coordinates:24°33'18" N, 9°29'06" E). Panel A displays the regional location of Algeria in North Africa; Panel B highlights the Wilaya of Djanet within Algeria; Panel C illustrates the detailed botanical collection site and regional landmarks. Geographic coordinates are reported in WGS 84 (EPSG:4326).

2.2. Reagents and Reference Standards

Methanol (MeOH), distilled water, hexane, petroleum ether, chloroform ($CHCl_3$), ethyl acetate (AcOEt), *n*-butanol (*n*-BuOH), ethanol (EtOH), and dimethyl sulfoxide (DMSO) were used as extraction and partitioning solvents. Analytical-grade reagents included anhydrous sodium sulfate (Na_2SO_4), sodium carbonate (Na_2CO_3), sodium bicarbonate ($NaHCO_3$), hydrochloric acid (HCl), sulfuric acid (H_2SO_4), sodium hydroxide (NaOH), potassium iodide (KI), sodium chloride (NaCl), magnesium turnings (Mg), ammonium hydroxide (NH_4OH), iodine (I_2), Dragendorff's reagent, ferric chloride ($FeCl_3$), Fehling's solutions, copper(II) sulfate ($CuSO_4$), Folin–Ciocalteu reagent, and aluminum chloride ($AlCl_3$). Gallic acid and quercetin were used as reference standards for the determination of total phenolic and total flavonoid contents, respectively.The *in vitro* antioxidant assays employed 2,2-diphenyl-1-picrylhydrazyl (DPPH), 2,2'-azino-bis(3-ethylbenzothiazoline-6-sulfonic acid) (ABTS), potassium persulfate ($K_2S_2O_8$), trichloroacetic acid (TCA), *o*-phenanthroline, butylated hydroxyanisole (BHA), butylated hydroxytoluene (BHT), ascorbic acid, and α-tocopherol. α-Glucosidase, 4-nitrophenyl α-D-glucopyranoside (4-NPG) and acarbose were used in the enzyme-inhibition assay, whereas -Mueller–Hinton agar and potato dextrose agar (PDA) were used for the antibacterial and antifungal assays, respectively.

2.3. Proximate analysis

Proximate parameters were determined in triplicate.

Moisture and dry matter

Powdered plant aliquots (P = 1.0 g) were weighed into pre-conditioned porcelain crucibles and dried in an oven at 105 °C to constant mass. Moisture content was calculated as: Moisture (%) = $[(M_1 - M_2)/P] \times 100$, where M_1 is the initial mass (crucible plus sample) and M_2 is the mass after drying. Dry matter (%) was obtained as 100 − moisture (%).

Total ash and organic matter

A 1.0 g sample was incinerated in a muffle furnace at 550–600 °C until a grayish-white residue was obtained, indicating complete destruction of organic matter. Total ash (%) was calculated as: Ash (%) = $[(M_1 - M_0)/P] \times 100$, where M_0 is the mass of the empty crucible and M_1 is the mass of the crucible containing the calcined residue. Organic matter (%) was calculated by subtracting total ash from dry matter.

Crude fat

A 1.0 g aliquot was placed in a cellulose thimble and extracted in a Soxhlet apparatus with 25 mL of *n*-hexane under continuous reflux for 1 h. The solvent was evaporated at 105 °C for 24 h, and the residue was cooled in a desiccator and weighed. Crude fat (%) was calculated relative to the initial test portion. All proximate parameters, except dry matter, were expressed as percentages of the initial sample mass (as-is basis), without correction for moisture content. Results are expressed as mean ± SD of three determinations.

2.4. Extraction and liquid–liquid fractionation

The extraction scheme is summarised in Figure 3. The dried powder (1000.34 g) was macerated at room temperature in methanol/water (70:30, v/v; 5 L per cycle, i.e. a solid-to-solvent ratio of about 1:5, g/mL) in three successive cycles of 72, 48 and 24 h, under periodic magnetic stirring and with renewal of the solvent at each cycle. The combined hydromethanolic extracts were filtered and concentrated under reduced pressure in a rotary evaporator at a temperature kept below 35 °C.

The concentrated aqueous residue 700 mLwas partitioned in a separating funnel, in sequence, against solvents of increasing polarity: petroleum ether, chloroform ($CHCl_3$), ethyl acetate (AcOEt) and *n*-butanol (*n*-BuOH), each applied as 3 × 24 h. Each organic phase was dried over anhydrous sodium sulfate (Na_2SO_4), filtered, evaporated to dryness under reduced pressure and weighed. The extracts weighed 0.23 g (petroleum ether), 8.05 g ($CHCl_3$), 4.23 g (AcOEt) and 23.50 g (*n*-BuOH). Yields were calculated relative to the starting powder (1000.34 g).

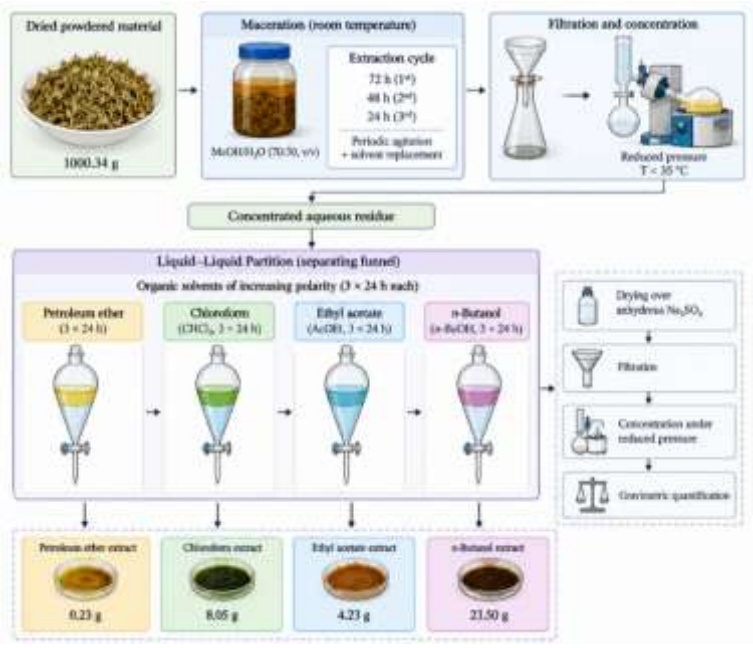


Figure 3: Schematic diagram of the bio-guided solvent partition procedure implemented on *Solenostemma argel* aerial parts.

2.5. Qualitative phytochemical screening

The four organic extracts and the residual aqueous phase were screened for selected phytochemical groups using qualitative colorimetric, precipitation and fluorescence tests, following established phytochemical methods with appropriate procedural adaptations (Harborne, 1998; Evans, 2009). The tests and their diagnostic observations are summarized in Table 1.

Table 1: Qualitative phytochemical screening tests and diagnostic reactions

Phytochemical group	Test and diagnostic observation	References
Flavonoids	Shinoda test; pink, crimson or magenta coloration.	Harborne (1998); Evans (2009).
Coumarins	Alkaline fluorescence test using NH_4OH; fluorescence examined at 365 nm.	Harborne (1998).
Alkaloids	Wagner's test (brown precipitate) and Dragendorff's test (orange to reddish-orange precipitate) after acidic extraction.	Evans (2009);Harborne (1998).
Saponins	Persistent foam test using distilled water and vigorous shaking.	Evans (2009).
Tannins	Ferric chloride test; dark green, blue-green or blue-black coloration.	Harborne (1998); Evans (2009).
Free reducingsugars	Fehling's test; brick-red Cu_2O precipitate after heating.	Evans (2009); WHO (2011).
Anthraquinones	Bornträger's test; pink to red coloration in the alkaline phase.	Harborne (1998); Evans (2009).
Sterols and triterpenes	Salkowski test; characteristic color change at the interface between the chloroform and sulfuric acid phases.	Harborne (1998); Evans (2009).
Proteins	Biuret test; violet coloration in an alkaline copper(II) medium.	Evans (2009); WHO (2011).

Note: Each organic extract and the residual aqueous phase should be tested separately. Record observations as positive (+), negative (−) or equivocal (±), using appropriate reagent blanks and positive controls. These screening tests provide preliminary evidence of phytochemical groups and do not establish the identity or concentration of individual compounds.

2.6. Total phenolic and flavonoid contents

Total phenolic content (TPC) was quantified spectrophotometrically using the Folin–Ciocalteu method adapted to a 96-well microplate format (Singleton & Rossi, 1965). An aliquot of 25 µL of extract dissolved in methanol (1.0 mg/mL) was mixed with 100 µL of Folin–Ciocalteu reagent pre-diluted 1:10 (v/v) in distilled water and 75 µL of 7.5% (w/v) sodium carbonate (Na_2CO_3). Following incubation in darkness for 2 h at room temperature, the optical density was measured at 765 nm against a blank. Gallic acid was employed to construct an eight-point calibration curve across the range of 25-200 µg/mL ($y = 0.0026x + 0.1824$); ($R^2 = 0.9738$). Where required, samples were appropriately diluted to align within the linear range of the calibration curve. TPC was expressed as micrograms of gallic acid equivalents per milligram of dry extract (µg GAE/mg).

Total flavonoid content (TFC) was estimated using the aluminium chloride ($AlCl_3$) colorimetric assay (Topçu et al., 2007). A volume of 1,000 µL of extract solution (1.0 mg/mL in methanol) was combined with 1,000 µL of 2% (w/v) methanolic $AlCl_3$. After 15 min of incubation at room temperature, absorbance was recorded at 430 nm. Quercetin was used as the calibration standard across a 25–200 µg/mL range ($y = 0.0048x$); ($R^2 = 0.997$). Results were expressed as micrograms of quercetin equivalents per milligram of dry extract (µg QE/mg).

Natural Resources for Human Health
eISSN: 2583-1194

2.7. *In Vitro* Biological Activities

2.7.1. *In vitro* antioxidant assays

The antioxidant activity of the $CHCl_3$, AcOEt, and *n*-BuOH extracts was evaluated in 96-well microplates across serial dilutions (12.5-800 µg/mL for DPPH and $ABTS^{\bullet+}$ assays and 1,10-phenanthroline assays). Synthetic and natural antioxidants, including butylated hydroxyanisole (BHA), butylated hydroxytoluene (BHT), ascorbic acid, and α-tocopherol, served as positive reference standards. Radical inhibition percentages (PI, %) were calculated as follows:

$$\mathrm{PI}\ (\%) = \left[\frac{A_{\mathrm{control}} - A_{\mathrm{sample}}}{A_{\mathrm{control}}}\right] \times 100$$

The half-maximal inhibitory concentration (IC_{50}) and the effective concentration corresponding to an absorbance of 0.50 ($A_{0.5}$) were determined from dose–response regression curves. (IC_{50}) values were used to characterize radical-scavenging activity, whereas ($A_{0.5}$) values were used to evaluate reducing power.

DPPH radical-scavenging assay. The assay was performed according to Blois (1958), with modifications for a 96-well microplate format. Briefly, 40 µL of extract solution or reference standard was mixed with 160 µL of methanolic DPPH solution (0.06 g/L; initial absorbance ≈ 0.50 at 517 nm). After incubation in the dark for 10 min at room temperature, the decrease in absorbance was measured at 517 nm. BHA and BHT were used as positive controls.

ABTS radical cation decolorization assay. The assay was carried out according to Re et al. (1999). The $ABTS^{\bullet+}$ radical cation was generated by mixing equal volumes of 7 mM aqueous ABTS solution and 2.45 mM potassium persulfate ($K_2S_2O_8$) solution. The mixture was kept in the dark at room temperature for 12-16 h before use. The resulting $ABTS^{\bullet+}$ solution was diluted with ethanol or distilled water to obtain an absorbance of approximately 0.70 at 734 nm. An aliquot of 40 µL of sample was mixed with 160 µL of the adjusted $ABTS^{\bullet+}$ solution and incubated for 10 min at room temperature. Absorbance was measured at 734 nm. BHA and BHT served as positive reference standards.

1,10-Phenanthroline ferric-reducing assay. Ferric-reducing activity was determined using the spectrophotometric method described by Szydłowska-Czerniak et al. (2008), adapted to a 96-well microplate format. Briefly, 10 µL of extract solution was mixed with 50 µL of 0.2% (w/v) $FeCl_3$, 30 µL of 0.5% (w/v) 1,10-phenanthroline in methanol, and 110 µL of methanol. After incubation at 30 °C for 20 min in the dark, absorbance was measured at 510 nm to monitor the formation of the orange-red Fe^{2+}-1,10-phenanthroline complex. BHA and BHT were used as reference antioxidants.

2.7.2. α-Glucosidase Inhibitory Activity

The inhibitory activity of the extracts against α-glucosidase was evaluated according to the method described by Palanisamy et al.*(* (2011), with slight modifications. Briefly, 50 µL of each extract at different concentrations (6.25µg/mL µg/ml - 400 µg/mL) was mixed with 50 µL of 4-nitrophenyl α-D-glucopyranoside (4-NPG, 5 mM) and 100 µL of α-glucosidase solution (0.1 U/mL). The reaction mixture was incubated at 37 °C for 15 min. Absorbance was recorded at 405 nm at the beginning of the reaction (0 min) and after incubation (15 min). A sample blank was prepared for each extract to correct for any background absorbance. Acarbose was used as a positive control and tested at different concentrations.The percentage of α-glucosidase inhibition was calculated using the following equation:

Inhibition (%) = [(Absorbance $_{\mathrm{Extract}}$ − Absorbance $_{\mathrm{Blank}}$) / Absorbance $_{\mathrm{Control}}$] × 100

$$\mathrm{Inhibition}\ (\%) = \left[\frac{A_{\mathrm{Extract}} - A_{\mathrm{Blank}}}{A_{\mathrm{Control}}}\right] \times 100$$

Control: Enzyme + substrate + extract solvent, Blank: Substrate + extract + enzyme buffer.

2.7.3. Antimicrobial assays

Antibacterial disc diffusion assay.

Antibacterial activity was evaluated against the Gram-positive bacterium *Staphylococcus aureus* (ATCC 25923) and the Gram-negative bacterium *Escherichia coli* (ATCC 25922) using the standardized disc diffusion method described by Bauer et al. (1966). Bacterial suspensions were prepared in sterile physiological saline and adjusted to a turbidity equivalent to a 0.5 McFarland standard before being uniformly spread onto Mueller–Hinton agar plates using sterile cotton swabs. Sterile Whatman N°. 3 filter paper discs (6 mm in diameter) were impregnated with 30 µL of each extract dissolved in dimethyl sulfoxide (DMSO) at concentrations of 0.625, 1.25, 2.5 and 5.0 mg/mL, corresponding to maximum extract loadings of 18.75, 37.5, 75 and 150 µg per disc, respectively. Discs impregnated with pure DMSO served as negative solvent controls. Following incubation at 37 °C for 24 h, inhibition zone diameters, including the 6 mm disc diameter, were measured in millimetres using a caliper. All assays were performed in triplicate.

Antifungal radial growth assay.

In vitro antifungal activity was assessed against the phytopathogenic fungus *Fusarium oxysporum* f. sp. *lycopersici* (ATCC 4287) using potato dextrose agar (PDA) composed of potato infusion (200 g/L), D-glucose (20 g/L) and agar (15 g/L). A 5 mm mycelial plug excised from the actively growing margin of a young fungal culture was aseptically placed at the centre of each Petri dish. Extract solutions prepared in DMSO at concentrations of 1.25, 2.5 and 5.0 mg/mL were applied at 40 µL per plate. Negative controls consisted of PDA plates without solvent, whereas solvent controls received 40 µL of pure DMSO. The plates were incubated at 25 °C for 24 h, after which radial mycelial growth was measured in millimetres.

The percentage inhibition of radial growth (I, %) was calculated as follows:

$$I\ (\%) = \left[\frac{C_{(T+)} - C_{(E)}}{C_{(T+)}}\right] \times 100$$

where (C(*T*+) represents radial mycelial growth (mm) in the DMSO solvent control and (C(*E*)) represents radial mycelial growth (mm) in the presence of the test extract.

2.8. Statistical analysis

All experimental determinations were performed in triplicate (n=3), and the results are expressed as mean ± standard deviation (SD). Data processing, curve fitting and linear or nonlinear regression analyses for the determination of (IC_{50}) and ($A_{0.5}$) values were performed using Microsoft Excel (Office 365) and GraphPad Prism (version 8.0). Where appropriate, differences among group means were assessed by one-way analysis of variance (ANOVA), followed by Tukey's post hoc test. Statistical significance was set at (P<0.05\).

3. RESULTS

3.1. Proximate composition of aerial parts

The proximate physicochemical composition of the aerial parts of *Solenostemma argel* is summarized in Table 2 (Figure 4). The plant material showed a moisture content of 10.39 ± 0.31%, corresponding to a dry matter content of 89.61 ± 0.31%. These values indicate a relatively low residual moisture content, which may favor storage stability under appropriate storage conditions. The total ash content was 3.99 ± 0.21%, while organic matter accounted for 85.62 ± 0.23% of the initial sample mass. Soxhlet extraction using *n*-hexane yielded a crude fat content of 1.64 ± 0.06%, indicating a relatively low proportion of hexane-extractable lipophilic constituents in the aerial parts of *S. argel*.

Table 2: Proximate composition of *Solenostemma argel* aerial parts (mean ± SD, *n* = 3).

Parameter	Replicate 1	Replicate 2	Replicate 3	Mean ± SD
Moisture content (%)	10.15	10.74	10.27	10.39 ± 0.31
Dry matter (%)	89.85	89.26	89.73	89.61 ± 0.31
Total ash (%)	3.97	3.80	4.21	3.99 ± 0.21
Organicmatter (%)	85.88	85.46	85.52	85.62 ± 0.23
Crude fat (%)	1.58	1.67	1.68	1.64 ± 0.06

Natural Resources for Human Health
eISSN: 2583-1194

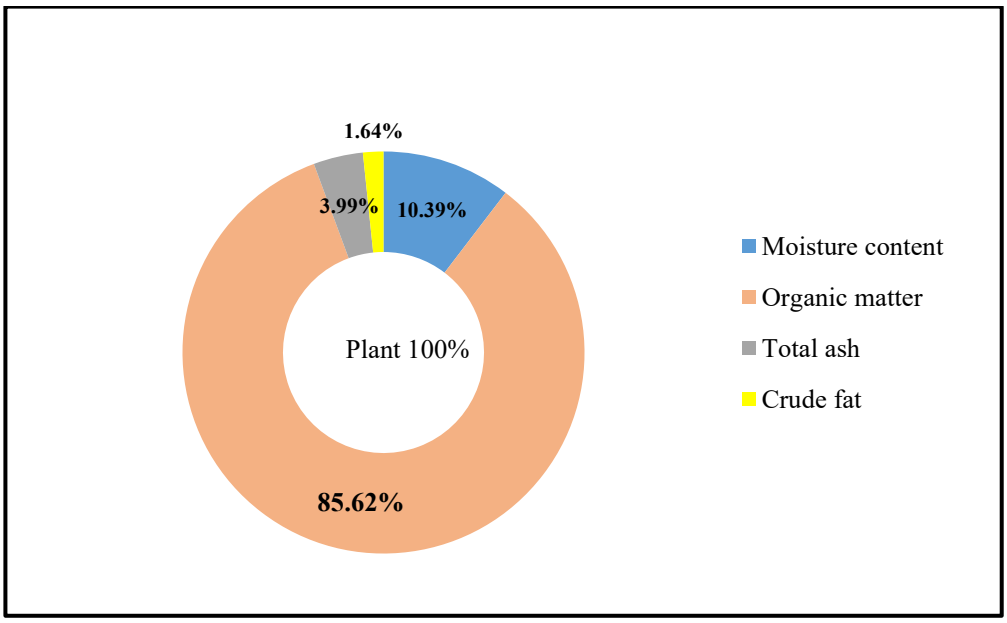


Figure 4: Proximate Composition of the *S. argel*%

3.2. Phytochemical profiling of solvent extracts

Qualitative phytochemical screening revealed a clear polarity-dependent distribution of secondary metabolites among the solvent extracts (Table 3). Flavonoids, alkaloids, and tannins were detected in all organic extracts, with the strongest reactions generally observed in the ethyl acetate and *n*-butanol extracts.

Saponins were absent from petroleum ether but detected in the chloroform, ethyl acetate, *n*-butanol, and residual aqueous extracts. Coumarins were detected only in the petroleum ether and ethyl acetate extracts. Sterols and triterpenes were abundant in the non-polar and medium-polarity extracts, particularly petroleum ether and chloroform. In contrast, anthraquinones, free sugars, and free proteins were not detected in any extract.

Table 3: Qualitative phytochemical screening of extracts from *Solenostemma argel* aerial parts.

Phytochemical class	Petroleum ether extract	$CHCl_3$ extract	EtOAc extract	*n*-BuOHextract	Residual aqueous
Flavonoids	+	+	++	+++	−
Alkaloids (Wagner/Dragendorff)	++ / ++	+ / +	+ / ++	+++ / +++	−
Tannins	+	+++	+++	++	−
Saponins	−	+	+	+	+
Coumarins	+	−	+	−	−
Sterols and triterpenes	+++	+++	+	+	−
Anthraquinones	−	−	−	−	−
Free sugars	−	−	−	−	−
Free proteins	−	−	−	−	−

(+++): abundant; (++): moderate; (+): trace; (−): not detected.

3.3. Total phenolic and flavonoid contents

The quantitative results (Table 4, figure 5) corroborated the qualitative screening data. The *n*-butanol extract exhibited the highest total phenolic content (TPC), with 339.33 ± 2.85 µg GAE/mg extract, followed closely by the ethyl acetate extract (324.46 ± 1.99 µg GAE/mg extract). The chloroform extract contained markedly lower phenolic levels (60.36 ± 2.29 µg GAE/mg extract).

A similar trend was observed for total flavonoid content (TFC). The highest value was recorded for the *n*-butanol extract (233.47 ± 1.87 µg QE/mg extract), followed by the ethyl acetate extract (218.06 ± 1.95 µg QE/mg extract), whereas the chloroform extract showed the lowest content (45.65 ± 0.88 µg QE/mg extract).

Table 4: Total phenolic and flavonoid contents of *Solenostemma argel* extracts (mean ± SD, *n* = 3).

Extract	TPC (µg GAE/mg extract)	TFC (µg QE/mg extract)
$CHCl_3$	60.36 ± 2.29	45.65 ± 0.88
EtOAc	324.46 ± 1.99	218.06 ± 1.95
***n*-BuOH**	339.33 ± 2.85	233.47 ± 1.87

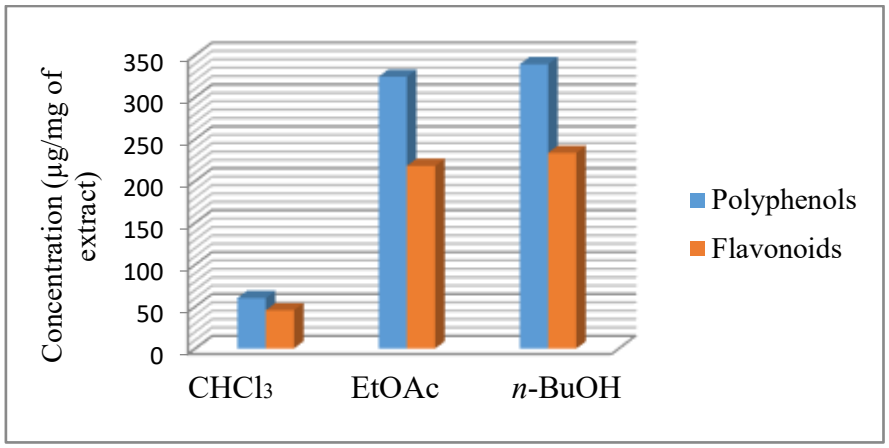


Figure 5: Total phenolic and total flavonoid contents in the three extracts of *S.argel*

3.4. *In vitro* antioxidant activity

The antioxidant potential of the extracts differed markedly according to the assay and solvent polarity (Table 5, figure 6). In the DPPH assay, the *n*-butanol extract was the most active plant extract, with an IC_{50} value of 76,70±3.41µg/mL and a maximum inhibition of 90.42±1.63% at 800 µg/mL.This was followed by the ethyl acetate extract, which showed comparable efficacy (IC_{50} = 83.33±2.52µg/mL), whereas the chloroform extract was weakly active (IC_{50}=121.15±0.35µg/mL).

Table 5: Antioxidant activity by the DPPH assay[a]

Concentrations / Extracts (µg/mL)	% Inhibition in DPPH Assay							IC_{50} (µg/ml)
	12.5	25	50	100	200	400	800	
$CHCl_3$ extract	6.53±3.14	9.75±2.19	21,47±5.10	41.68±2.55	69.61±3.20	83.37±1.09	83.37±0.36	121.15±0.35
EtOAc extract	16.45±1.4	23.17±2.3	35.73±2.5	56.43±3.3	78.41±2.8	87.55±1.3	90.20±0.6	83.33±2.52

	8	0	8	3	1	8	7	
***n*-BuOH extract**	14.41±4.63	22.67±0.92	39.31±1.06	59.30±2.36	80.50±1.79	89.54±0.19	90.42±1.63	76,70±3.41
BHA[b]	76.55±0.48	79.89±0.26	81.73±0.10	84.18±0.10	87.13±0.17	89.36±0.19	90.14±0.00	6.14±0.41
BHT[b]	49.09±0.76	72.63±2.06	88.73±0.89	94.00±0,31	94.97±0.08	95.38±0.41	95.02±0.23	12.99±0.41

[a]Values expressed as means ± S.D of three parallel measurements. (p <0.05).

[b]Reference compounds.

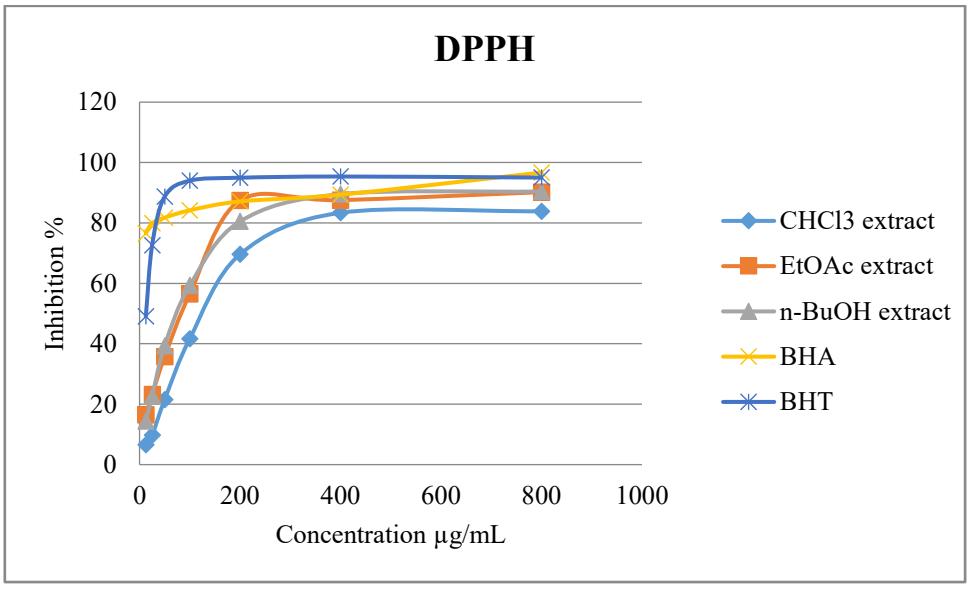


Figure 6: DPPH radical scavenging activity of the three extracts, BHA and BHT at different concentrations. (mean ±SD, n=3).

In the ABTS radical cation decolorization assay (Table 6, figure 7), the *n*-butanol extract also exhibited the strongest activity (53.45±1.07 µg/mL), followed by the ethyl acetate extract (IC_{50} = 86.85±1.24µg/mL). Both extracts inhibited more than 90% of the ABTS radicals at a concentration of 800 µg/mL. The chloroform extract, by contrast, was the least effective (IC_{50} = 127.69±2,32µg/mL).

Table 6: Antioxidant activity by the ABTS assay[a].

Concentrations Extracts (µg/mL)	**% Inhibition in ABTS Assay**							**IC_{50} (µg/ml)**
	12.5	**25**	**50**	**100**	**200**	**400**	**800**	
$CHCl_3$ extract	7.33±1.15	9.64±3.10	22,41±2.10	40.36±0.50	75.18±1.26	81.22±0.09	83.23±0.14	127.69±2,32
EtOAcextract	15..33±1.0	22. 07±1.4	35.63±1.6	55.13±1.2	79,11±1,8	83.12±1.3	90.22±0.1	86.85±1.24

Natural Resources for Human Health
eISSN: 2583-1194

	8		8	2	1	1	7	
***n*-BuOH extract**	24.41±1.23	32.67±0.13	49.31±0.17	58.59±2.13	80.49±0.15	90.54±1.16	92.42±0.25	53.45±1.07
BHT[b]	69.21±0.40	78.23±1.34	88.12±1.28	88.76±3.07	90.85±1.74	90.95±0.51	96.68±0.39	1.29±0.30
BHA[b]	92.83±1.42	94.68±0.42	94.95±0.90	95.32±0.25	95.59±0.47	95.83±0.15	95.86±0.10	1.81±0.10

[a]Values expressed as means ± S.D of three parallel measurements. (p <0.05).

[b]Reference compounds

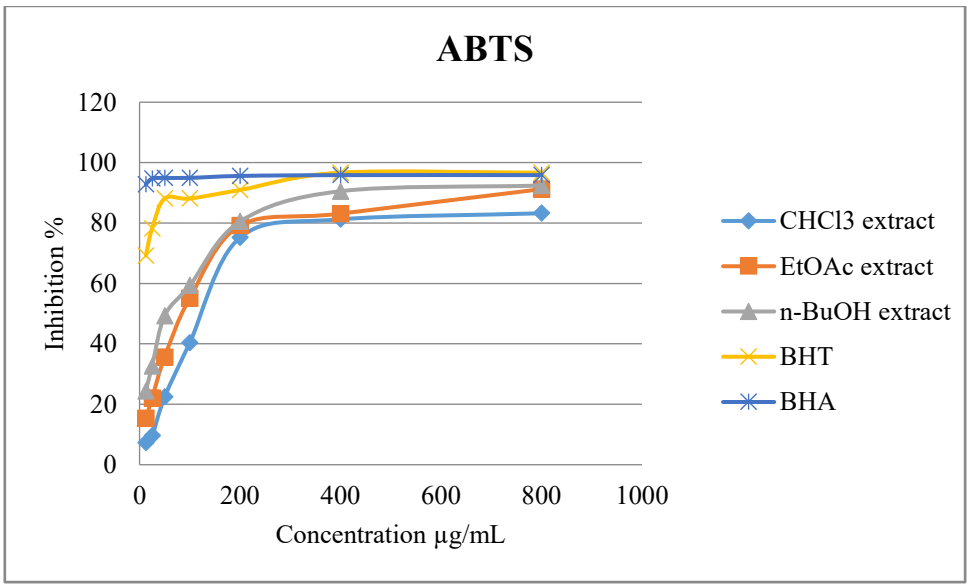


Figure 7:ABTS activity of the three extracts, BHA, BHT at different concentrations. (mean ±SD, n=3).

In the phenanthroline assay (Table 7, figure 8), both the *n*-butanol and ethyl acetate extracts demonstrated strong reducing capacity, with $A_{0.50}$ values of 58.33±0.38 and 57.14±1.13 µg/mL, respectively, whereas the chloroform extract remained inactive under the tested conditions.

Table 7: Antioxidant activity by phenanthroline assay[a].

Concentration (µg/ml)Extracts	**Absorbance**							**$A_{0.50}$**
	3.125	**6.25**	**12.5**	**25**	**50**	**100**	**200**	
$CHCl_3$ extract	0.20±0.05	0.26±0,08	0.23±0.06	0.23±0.02	0.25±0.07	0.28±0.05	0.41±0.02	>200
AcOEt extract	0.25±0.04	0.27±0.01	0.31±0.03	0.35±0.01	0.45±0.06	0.76±0.07	1.61±0.26	57.14±1.13
***n*-BuOH extract**	0.26±0.00	0.25±0.03	0,30±0.01	0.36±0.03	0.48±0.01	0.75±0.07	1.36±0.18	58.33±0.38
BHA[b]	0.49±0.01	0.59±0.01	0.73±0,02	0.93±0.01	1.25±0.04	2.10±0.05	4.89±0.06	0.93±0.07
BHT[b]	0.47±0.01	0.47±0,01	0.53±0,03	1.23±0.02	1.84±0.01	3.48±0.03	4.84±0.01	2.24±0.17

[a]Values expressed as means ± S.D of three parallel measurements. (p <0.05).

[b]Reference compounds

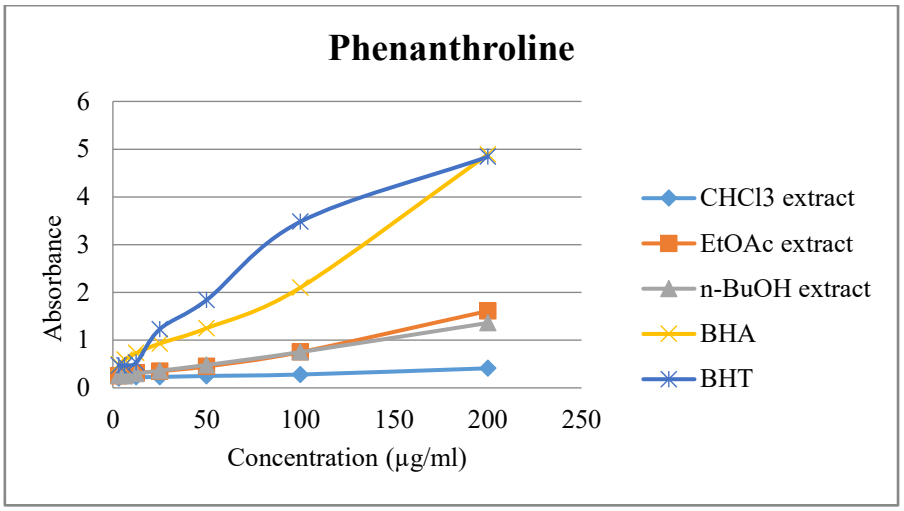


Figure 8: Phenanthroline activity of the three extracts, BHA, BHT at different concentrations. (mean ±SD, n=3).

3.5. α-Glucosidase Inhibition Assay

The α-glucosidase inhibitory activity differed markedly among the three extracts (Table 8). The chloroform extract showed the highest activity, achieving 61.17 ± 1.11% inhibition at 400 µg/mL, with an IC_{50} of 164 ± 0.50 µg/mL. By comparison, the ethyl acetate and *n*-butanol extracts exhibited limited activity, with inhibition rates of 7.71 ± 1.68% and 3.14 ± 1.38%, respectively, at the maximum tested concentration. Notably, the chloroform extract displayed a lower IC_{50} than acarbose (275.43 ± 1.59 µg/mL), suggesting a stronger α-glucosidase inhibitory potential under the experimental conditions used.

Table 8: α-Glucosidase Inhibitory activity of the three extracts of *Solenostemma argel*

	% α-Glucosidase Inhibitory activity							
Extracts	6.25µg/mL	12.5µg/mL	25µg/mL	50µg/mL	100µg/mL	200µg/mL	400µg/mL	IC_{50}(µg/mL)
$CHCl_3$ extract	11.06±0.13	26.08±0.12	28.04±0.15	33.02±0.13	43.59±0.04	53.04±1.12	61.17±1.11	164±0.50
EtOAc extract	NA	2,13±0.14	2.58±0.17	3.41±0.31	3.59±0.34	6.31±1.02	7.71±1.68	> 400
***n*-BuOH extract**	NA	NA	NA	NA	0.48±0.19	1.99±0.54	3.14±1.38	> 400
Acarbose[b]	78. 125 µg/mL	156. 25 µg/mL	312.5 µg/mL	625 µg/mL	1250 µg/mL	2500 µg/mL	5000 µg/mL	IC_{50}µg/mL
	27.43±2.18	38.91±3.20	54.86±1.799	67.29±2.63	80.19±1.66	85.54±0.45	91.05±0.72	275.43±1.59

NA: not active

3.6. Antimicrobial activity

The antibacterial activity of *Solenostemma argel* extracts varied depending on the bacterial strain and extract type (Table 9). Against *Escherichia coli* ATCC 25922, the ethyl acetate (EtOAc) extract showed the strongest activity, with a maximum inhibition zone of 17 ± 0.0 mm at 5.0 mg/mL, followed by the chloroform ($CHCl_3$) extract (15 ± 0.7 mm). In contrast, the petroleum ether extract showed the strongest activity against *Staphylococcus aureus* ATCC 25923, with an inhibition zone of 14 ± 0.5 mm, whereas the other extracts showed no inhibitory activity against this bacterium.

Table 9: Antibacterial activity of *Solenostemma argel* extracts, expressed as inhibition zone diameters (mm).

Bacterial strain	**Extracts Concentration**	**Zone of inhibition (mm)**			
		0.625mg/mL	1.25 mg/mL	2.5 mg/mL	5 mg/mL
***Escherichia coli* ATCC 25922**	Petroleum ether	NI	NI	9±0.5	9±0.4
	$CHCl_3$	8±0.7	14±0.5	15±0.4	15±0.7
	EtOAc	10±0.1	13±0.5	14±0.7	17±0.0
	n-BuOH	8±0.1	9±0.1	9±0.4	12±0.7
***Staphylococcus aureus* ATCC 25923**	Petroleum ether	NI	12±0.1	12±0.4	14±0.5
	$CHCl_3$	NI	NI	NI	NI
	EtOAc	NI	NI	NI	NI
	n-BuOH	NI	NI	NI	NI

Zone of inhibition diameters include the diameter of the paper discs (6 mm) and are expressed as mean ± standard deviation. NI: no inhibitory effect

All extracts exhibited antifungal activity against *Fusarium oxysporum* f. sp. *lycopersici* (Table 10). The highest mycelial growth inhibition was observed at 5 mg/mL for the ethyl acetate and chloroform extracts, reaching 41.67% and 40.38%, respectively. The *n*-butanol extract showed a lower inhibition rate of 27.56% at the same concentration.

Table 10: Antifungal activity of *Solenostemmaargel*extracts against *Fusarium oxysporum* f. sp. *lycopersici*.

Concentration	1.25 mg/mL		2.5 mg/mL		5 mg/mL	
Extract	Radial growth(mm)	Inhibition (%)	Radial growth(mm)	Inhibition (%)	Radial growth(mm)	Inhibition (%)
$CHCl_3$	12.5±0.5	19.87	10.6±0.4	32.05	9.3±0.7	40.38
EtOAc	12.6±0.4	19.23	11.5±0.0	26.28	9.1±0.4	41.67
***n*-BuOH**	13.0±0.7	16.67	12.3±0.1	21.15	11.3±0.2	27.56
C – 17.6 mm (PDA), *S* -15.6 mm (PDA + DMSO)						

C- : Negative control, *S*:-Solvent control

4. DISCUSSION

Medicinal shrubs growing in Saharan environments develop physiological and biochemical adaptations to counter severe heat, prolonged drought, and intense ultraviolet radiation. The low moisture content observed in *S. argel* aerial parts (10.39 ±

0.31%) falls within the recommended pharmacological range (< 12-14%) required to limit enzymatic degradation and prevent microbial spoilage during dry storage. The substantial dry matter (89.61 ± 0.31%) and organic matter (85.62 ± 0.23%) underline an integrated carbon matrix rich in structural macromolecules and specialized protective metabolites. Furthermore, the total ash content (3.99 ± 0.21%) reflects physiological mineral uptake suited for osmotic adjustment in desert soils without excessive hyper-saline accumulation. The partition of aerial biomass across four organic solvent systems revealed a clear polarity-dependent distribution of specialized metabolites. The preferential accumulation of phenolics and flavonoids in the polar n-butanol (339.33 µg GAE/mg; 233.47 µg QE/mg) and ethyl acetate (324.46 µg GAE/mg; 218.06 µg QE/mg) phases aligns with general extraction equilibria established for Saharan angiosperms. In these systems, polyhydroxylated flavonoids, phenolic acids, and their glycosylated congeners partition selectively into solvents with high dielectric constants and hydrogen-bonding capacity (Aliouche et al., 2022). Conversely, low-polarity lipophilic compounds, non-polar triterpenoids, and phytosterols migrate into the petroleum ether and chloroform layers, as confirmed by positive Salkowski reactions.

The *in vitro* antioxidant assays (DPPH, $ABTS^{\bullet+}$ and phenanthroline) revealed that the *n*-BuOH and AcOEt extracts exhibited stronger antioxidant activity than the $CHCl_3$ extract. This difference may be related to their higher phenolic and flavonoid contents, as these compounds are known to contribute to free-radical scavenging. Elsanhoty et al. (2022) reported DPPH IC_{50} values of 124.20 ± 6.40 µg/mL for the ethyl acetate extract and 26.10 ± 17.40 µg/mL for the chloroform extract. In the present study, the *n*-BuOH and AcOEt extracts showed better activity, with IC_{50} values of 76.70 ± 3.41 and 83.33 ± 2.52µg/mL, respectively, while $CHCl_3$ exhibited weaker activity (121.15 ± 0.35 µg/mL). The ABTS assay confirmed this trend, with IC_{50} values of 53.45 ± 1.07., 86.85 ± 1.84 and 127.69 ± 2.32 µg/mL for *n*-BuOH, AcOEt and $CHCl_3$, respectively. The differences compared with Elsanhoty et al. (2022) may be related to the extraction procedures: they used each solvent independently, whereas the present study involved successive liquid–liquid partitioning of a hydroethanolic extract. Geographical origin and environmental conditions may also influence the plant's phytochemical composition and antioxidant activity.Benmaarouf et al. (2020) reported a DPPH IC_{50} of 36.05 ± 2.77 µg/mL for an acetone extract of Algerian *S. argel*, attributing its activity to flavonols such as rutin, kaempferol-3-O-rutinoside and astragalin. Compared with this extract, our *n*-BuOH fraction showed lower activity (52.45 ± 3.41 µg/mL). Nevertheless, Innocenti et al. (2005) also reported kaempferol glycosides in this species, supporting the contribution of flavonoids to its antioxidant potential.The phenanthroline assay further confirmed the activity of the polar fractions, with $A_{0.50}$ values of 57.14 ± 1.13 µg/mL for AcOEt and 58.33 ± 0.38 µg/mL for *n*-BuOH, whereas $CHCl_3$ showed considerably weaker reducing power ($A_{0.50}$> 200 µg/mL). Differences between DPPH and ABTS results may reflect the distinct reaction mechanisms and sensitivities of these assays towards antioxidant compounds (Re et al., 1999; Prior et al., 2005). Overall, these findings highlight the influence of extraction procedures and geographical origin on the antioxidant potential of *S. argel*.

Interestingly, the α-glucosidase inhibition assay revealed a distinct activity profile compared with the antioxidant results. While the flavonoid-rich *n*-BuOH and AcOEt extracts exhibited weak or negligible inhibitory effects, the $CHCl_3$ extract showed concentration-dependent inhibition, with an IC_{50} value of 164 ± 0.50 µg/mL, indicating greater inhibitory potency than the reference drug acarbose (IC_{50} = 275.43 ± 1.59 µg/mL) under the tested conditions. This activity may be partly associated with the phytochemical composition of the $CHCl_3$ extract. Indeed, qualitative screening (Table 3) revealed a high abundance of sterols and triterpenes (+++) in this fraction, compared with their lower presence (+) in the AcOEt and *n*-BuOH extracts and their absence in the residual aqueous fraction. This hypothesis is supported by previous studies demonstrating the α-glucosidase inhibitory potential of several triterpenoid compounds. Ouyang et al. (2018) reported that several pentacyclic triterpenoids isolated from *Akebia trifoliata* exhibited significant inhibitory activity against α-glucosidase, with some compounds showing greater potency than acarbose. Similarly, Bian et al. (2021) demonstrated the strong inhibitory effects of hederagenin, 3-epiakebonoic acid and arjunolic acid against this enzyme. Collectively, these findings suggest that triterpenoid constituents may contribute, at least partially, to the α-glucosidase inhibitory activity observed in the $CHCl_3$ fraction of *S. argel*. These results highlight the potential of *S. argel* as a source of natural α-glucosidase inhibitors, which may contribute to its traditional use in managing postprandial blood glucose levels. However, further phytochemical investigations are required to identify the compounds responsible for this activity.

The antimicrobial activity of *S. argel* varied according to the extract and the tested microorganism. The EtOAc extract showed the strongest activity against *E. coli* (17 ± 0.0 mm) and *Fusarium oxysporum* (41.67 % inhibition), while petroleum ether was the

most effective against *S. aureus* (14 ± 0.5 mm). The relatively high activity of EtOAc may be associated with its high tannin (+++) and moderate flavonoid (++) content, whereas the activity of $CHCl_3$ may partly be related to its high tannin, sterol and triterpene contents (+++) (Table 3). Interestingly, despite its high flavonoid content (+++), the *n*-BuOH extract exhibited weaker antimicrobial activity, suggesting that these effects depend on the combined contribution of different phytochemical constituents rather than flavonoids alone.

5. CONCLUSION

This study provides a comparative investigation of the proximate composition, solvent-extractated phytochemical profiles, multi-pathway antioxidant properties, and biological potential of *Solenostemma argel* (Delile) Hayne harvested from the Djanet region in the Algerian Sahara. Extractation using solvents of increasing polarity effectively segregated the bioactive pool: the polar *n*-butanol and ethyl acetate extracts concentrated high levels of polyphenols and flavonoids, demonstrating sustained radical-scavenging and iron-reducing capacities across DPPH, $ABTS^{\bullet+}$and phenanthroline assays. In contrast, the medium-polarity chloroform extract exhibited selective *in vitro* alpha- glucosidase inhibition, highlighting its interest for further antidiabetic research. The antimicrobial activity of *S. argel* was extract- and microorganism-dependent, potentially reflecting the contribution of different phytochemical constituents.

LIMITATIONS AND PERSPECTIVES:

The primary limitation of this work is the absence of chromatographic isolation and spectroscopic elucidation (HPLC-DAD, LC-MS, and NMR) of the individual molecules responsible for the observed activities. Future studies should focus on bioassay-guided isolation of the chloroform and butanol extracts to identify the active chemical structures and investigate their modes of action in validated cellular and *in vivo* models.

DECLARATIONS

- Author Contributions: Lamia Aliouche, Hanène Zater, and Souad Hamimed contributed to the methodology, investigation, and data acquisition. Lamia Aliouche conceptualized the research framework and supervised the project. Sara Mokhtari contributed to data interpretation and manuscript review. All authors reviewed and approved the final version of the manuscript.
- Funding: This study received no dedicated external research grant and was conducted within the academic research framework of University of Constantine 1 Frères Mentouri, and CRBT (Constantine. Algeria).
- Conflicts of Interest: The authors declare no conflict of interest regarding the publication of this manuscript.
- Data Availability Statement: All data generated or analyzed during this study are included within this article.

REFERENCES

[1] Aliouche, L., Larguet, H., Amrania, A., León, F., Brouard, I., Benayache, S., Zamaa, D., Meraihib, Z., & Benayache, F. (2018). Isolation, antioxidant and antimicrobial activities of ecdysteroids from *Serratulacichoracea*. *Current Bioactive Compounds*, 14, 60–66. DOI:10.2174/1573407214666171211154922

[2] Aliouche, L., Zater, H., Bicha, S., Benayache, S., Bensouici, C., Seghiri, R., &Benayache, F. (2022). *In vitro* antioxidant, anti-Alzheimer and antidiabetic activities, phenolic and flavonoid contents of different polarity extracts from *Serratulacichoracea* (DC.) (Asteraceae) aerial parts. Advances in Bioresearch, 13(2), 25–35. DOI:10.15515/abr.0976-4585.13.2.2535

[3] Bauer, A. W., Kirby, W. M. M., Sherris, J. C., &Turck, M. (1966). Antibiotic susceptibility testing by a standardized single disk method. *American Journal of Clinical Pathology*, 45(4), 493–496. https://doi.org/10.1093/ajcp/45.4_ts.493

[4] Benmaarouf, D. K., Pinto, D. C. G. A., China, B., Zenia, S., Bendesari, K. B., & Ben-Mahdi, M. H. (2020). Chemical analysis, antioxidant, anti-inflammatory and antinociceptive effects of acetone extract of Algerian *Solenostemma argel* (Delile) Hayne leaves. *International Journal of Current Pharmaceutical Research*, 12(5), 45–51. https://doi.org/10.22159/ijcpr.2020v12i5.39768

[5] Bian, G., Yang, J., Elango, J., Wu, W., Bao, B., & Bao, C. (2021). Natural triterpenoids isolated from *Akebia trifoliata* stem explants exert a hypoglycemic effect via α-glucosidase inhibition and glucose uptake stimulation in insulin-resistant HepG2 cells. *Chemistry & Biodiversity, 18*(5), e2001030. https://doi.org/10.1002/cbdv.202001030

[6] Blois, M. S. (1958). Antioxidant determinations by the use of a stable free radical. *Nature*, 181(4617), 1199–1200. https://doi.org/10.1038/1811199a0

[7] Boudjerda, A., Zater, H., Benayache, S., Chalchat, J.-C., González-Platas, J., León, F., Brouard, I., Bermejo, J., & Benayache, F. (2008). A new guaianolide and other constituents from *Achillealigustica*. *Biochemical Systematics and Ecology*, 36(5–6), 461–466. https://doi.org/10.1016/j.bse.2007.11.006

[8] El-Shiekh, R. A., Al-Mahdy, D. A., Mouneir, S. M., Hifnawy, M. S., & Abdel-Sattar, E. A. (2019). In vitro screening of selected traditional Egyptian plants for their anti-obesity and antioxidant activities and active extract exploration of *Solenostemmaargel*. *Journal of Traditional and Complementary Medicine*, 10(4), 391–401. https://doi.org/10.1016/j.jtcme.2019.06.002

[9] Elsanhoty, R. M., Soliman, M. S. M., Khidr, Y. A., Hassan, G. O. O., Hassan, A. R. A., Aladhadh, M., &Abdella, A. (2022). Pharmacological activities and characterization of phenolic and flavonoid compounds in *Solenostemma argel* extract. *Molecules*, 27(23), 8118. https://doi.org/10.3390/molecules27238118

[10] Evans, W. C. (2009). *Trease and Evans' Pharmacognosy* (16th ed.). Saunders Elsevier.

[11] Hamimed, S., Boulebda, N., Laouer, H., &Belkhiri, A. (2018). Bioactivity-guided isolation of alkamides from a cytotoxic extract of the ethyl acetate extract of *Anacyclus pyrethrum* (L.) DC. roots. *Current Issues in Pharmacy and Medical Sciences*, 31(4), 180–185. https://doi.org/10.1515/cipms-2018-0033

[12] Hammiche, V., &Maiza, K. (2006). Traditional medicine in Central Sahara: Pharmacopoeia of TassiliN'ajjer. *Journal of Ethnopharmacology*, 105(3), 358–367. https://doi.org/10.1016/j.jep.2005.11.028

[13] Harborne, J. B. (1998). *Phytochemical Methods: A Guide to Modern Techniques of Plant Analysis* (3rd ed.). Chapman & Hall. https://doi.org/10.1007/978-94-009-5570-7

[14] Innocenti, G., Dall'Acqua, S., Sosa, S., Altinier, G., &Della Loggia, R. (2005). Topical anti-inflammatory activity of *Solenostemma argel* leaves. *Journal of Ethnopharmacology*, 102(2), 307–310. https://doi.org/10.1016/j.jep.2005.06.007

[15] Ksouri, R., Megdiche, W., Debez, A., Falleh, H., Grignon, C., & Abdelly, C. (2012). Halophytes and extremophile plants as a promising source of antioxidant, antimicrobial and anti-inflammatory compounds. *Comptes Rendus Biologies*, 335(4), 282–291. https://doi.org/10.1016/j.crvi.2012.04.007

[16] López-Rodríguez, M., García, V. P., Zater, H., Benayache, S., &Benayache, F. (2009). Cynaratriol, a sesquiterpene lactone from *Centaurea musimomum*. *Acta Crystallographica Section E*, E65(8), o1867–o1868. https://doi.org/10.1107/S1600536809026701

[17] Mokhtari, S., Kheroua, O., Saidi D. (2016). Isolation and identification of lactic acid bacteria from Algerian durum wheat (*Triticum durum*) natural fermented in underground silos Matmora "El-Hammoum" and their antimicrobial activity against pathogenic germs. *Journal of Nutrition and Health Sciences* ,3(4),403. https://doi.org/10.15744/2393-9060.3.403

[18] Mokhtari, S., Bensouici, C., Saidi, D., & Kheroua, O. (2020a). Comparative study of antioxidant and anticholinesterase activity of unfermented and fermented wheat and couscous from fermented wheat "El Hammoum", traditional Algerian product. *Advances in Bioresearch*, 11(2), 40–50. https://doi.org/10.15515/abr.0976-4585.11.2.4050

[19] Mokhtari, S., Taghouti, M., Saidi ,D., Kheroua, O. (2020b). Traditional Algerian fermented food: first data on nutritional characteristics of wheat (*Triticum durum*) fermented in underground silos Matmor (Mascara, Algeria) compared to unfermented wheat. *Advances in Biology and Earth Sciences*. 2020, 5(3),176-192.

[20] Ouyang, J. K., Dong, L. M., Xu, Q. L., Wang, J., Liu, S. B., Qian, T., Yuan, Y. F., & Tan, J. W. (2018). Triterpenoids with α-glucosidase inhibitory activity and cytotoxic activity from the leaves of *Akebia trifoliata*. *RSC Advances, 8*, 40483–40489. https://doi.org/10.1039/C8RA08894B

[21] Ozenda, P. (2004). *Flore et végétation du Sahara* (3rd ed.). CNRS Éditions, Paris, France.

[22] Palanisamy, U. D., Ling, L.T., Manaharan, T., Appleton D. (2011). Rapid isolation of geraniin from *Nephelium lappaceum* rind waste and its anti-hyperglycemic activity. *Food Chemistry*, 127(1): 21-27. doi:10.1016/j.foodchem.2010.12.070.

[23] Peel, M. C., Finlayson, B. L., & McMahon, T. A. (2007). Updated world map of the Köppen-Geiger climate classification. *Hydrology and Earth System Sciences*, 11(5), 1633–1644. https://doi.org/10.5194/hess-11-1633-2007

[24] Perrone, A., Plaza, A., Ercolino, S. F., Hamed, A. I., Piacente, S., & Pizza, C. (2008). Seco- and normal-pregnane glycosides from *Solenostemma argel* and their antiproliferative activity. *Journal of Natural Products*, 71(12), 2003–2010. https://doi.org/10.1021/np800473x

[25] Plants of the World Online (POWO). (2026). *Plants of the World Online*. Royal Botanic Gardens, Kew. https://powo.science.kew.org/

[26] Plaza, A., Perrone, A., Ercolino, S. F., Hamed, A. I., Piacente, S., & Pizza, C. (2005). Argelosides A–J, 14,15-secopregnane glycosides from *Solenostemmaargel*. *Journal of Natural Products*, 68(11), 1642–1647. https://doi.org/10.1021/np050302y

[27] Prior, R. L., Wu, X., &Schaich, K. (2005). Standardized methods for the determination of antioxidant capacity and phenolics in foods and dietary supplements. *Journal of Agricultural and Food Chemistry*, 53(10), 4290–4302. https://doi.org/10.1021/jf0502698

[28] Quézel, P., & Santa, S. (1962–1963). *Nouvelle flore de l'Algérie et des régions désertiques méridionales* (Vols. 1–2). Éditions du Centre National de la Recherche Scientifique, Paris, France.

[29] Re, R., Pellegrini, N., Proteggente, A., Pannala, A., Yang, M., &Rice-Evans, C. (1999). Antioxidant activity applying an improved ABTS radical cation decolorization assay. *Free Radical Biology and Medicine*, 26(9-10), 1231–1237. https://doi.org/10.1016/S0891-5849(98)00315-3

[30] Shafek, R. E., & Michael, H. N. (2012). Antibacterial and antioxidant activity of two new kaempferol glycosides isolated from *Solenostemma argel* stem extract. *Asian Journal of Plant Sciences*, 11(3), 143–148. https://doi.org/10.3923/ajps.2012.143.148

[31] Singleton, V. L., & Rossi, J. A. (1965). Colorimetry of total phenolics with phosphomolybdic–phosphotungstic acid reagents. *American Journal of Enology and Viticulture*, 16(3), 144–158. https://doi.org/10.5344/ajev.1965.16.3.144

[32] Szydłowska-Czerniak, A., Dianoczki, C., Recseg, K., Karlovits, G., &Szłyk, E. (2008). Determination of antioxidant capacities of vegetable oils by ferric-ion spectrophotometric methods. *Talanta*, 76(4), 899–905. https://doi.org/10.1016/j.talanta.2008.04.055

[33] Taha, L. E., &Bakhit, S. M. (2014). The anti-hyperglycemic effect of *Solenostemma argel* compared with Glibenclamide. *International Journal of Advanced Research*, 2(1), 1–10.

[34] Topçu, G., Ay, M., Bilici, A., Sarıkürkcü, C., Öztürk, M., &Ulubelen, A. (2007). A new flavone from antioxidant extracts of *Pistaciaterebinthus*. *Food Chemistry*, 103(3), 816–822. https://doi.org/10.1016/j.foodchem.2006.09.028

[35] World Health Organization. (2011). *Quality Control Methods for Herbal Materials*. WHO Guidelines. World Health Organization, Geneva.

[36] World Meteorological Organization. (2021). *WMO Guidelines on the Calculation of Climate Normals (1991–2020)*. WMO-No. 1203, Geneva, Switzerland.

[37] Zater, H., Boudjerda, A., Huet, J., Oliveira Ribeiro, S., Benayache, S., Fontaine, V., Stévigny, C., Duez, P., &Benayache, F. (2014). Antimicrobial effects of aerial parts from Algerian centaury. *Planta Medica*, 80(16), 1442 (P1L96). https://doi.org/10.1055/s-0034-1394753

[38] Zater, H., Huet, J., Fontaine, V., Benayache, S., Stévigny, C., Duez, P., & Benayache, F. (2016). Chemical constituents, cytotoxic, antifungal and antimicrobial properties of *Centaurea diluta* Ait. subsp. *algeriensis* (Coss. &Dur.) Maire. *Asian Pacific Journal of Tropical Medicine*, 9(6), 554–561. https://doi.org/10.1016/j.apjtm.2016.04.016

[39] Zater, H., Rebbas, K., Bicha, S., & Bensaid, S. O. (2019a). Discovery of *Centaurea hyalolepis*Boiss. (Asteraceae) in the region of Djelfa. *Acta Botanica Malacitana*, 44, 67–69. https://doi.org/10.24310/abm.v44i0.5334

[40] Zater, H., Rebbas, K., Bicha, S., & Bensaid, S. O. (2019b). *Centaurea hyalolepis*Boiss. (Asteraceae). *CABI Compendium*. https://doi.org/10.1079/cabicompendium.113063

[41] Zater, H., Aliouche, L., Benayache, S., Chalchat, J.-C., Chalard, P., Figueredo, G., &Benayache, F. (2021). Chemical composition and in vitro evaluation of the antibacterial activity of the essential oil of the aerial parts of *Centaurea calitrapa* (Desf.) (Asteraceae) from the North-East region of Algeria. *Advances in Bioresearch*, 12(6), 1–9. https://doi.org/10.15515/abr.0976-4585.12.6.109

SUPPLEMENTARY MATERIAL

Table1: Overall results of the phytochemical screening of the petroleum ether extract

Secondarymetabolites Petroleum etherextract		Observation	
		Before	After
Flavonoids			
Coumarins			
Alkaloids	Wanger's test		
	dragendorff's test		
Saponins			

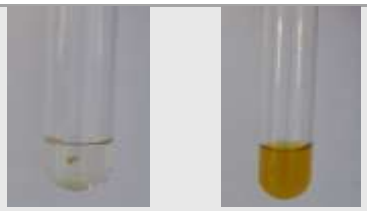
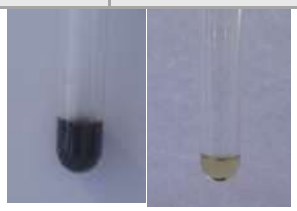
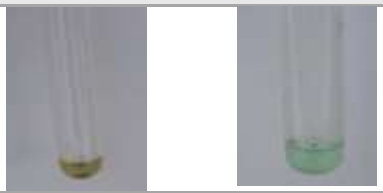
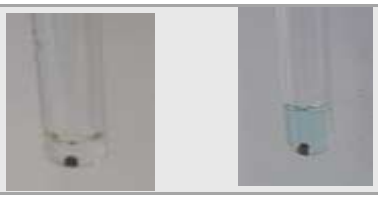
Tannins	
Sugars	
Anthraquinones	
Sterols	
Proteins	

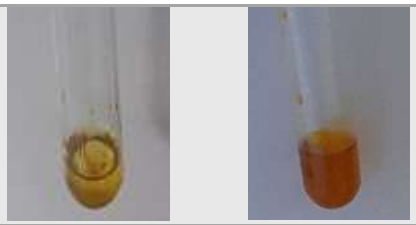
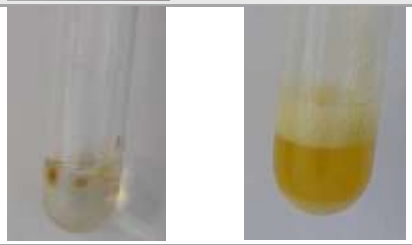
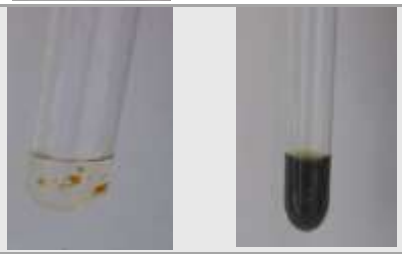
Table 2: Overall results of the phytochemical screening of the $CHCl_3$ extract

Secondarymetabolites $CHCl_3$extract	Obsrvation	
	Before	After
Flavonoids		
Coumarins		

Alkaloids	Wanger's test	
	dragendorff's test	
Saponins		
Tannins		
Sugars		
Anthraquinones		
Sterols		
Proteins		

Natural Resources for Human Health
eISSN: 2583-1194

Table 3: Overall results of the phytochemical screening of EtOAc extract

Secondary metabolites EtOAc extract		Observation	
		Before	After
Flavonoids			
Coumarins			
Alkaloids	Wanger's test		
	Dragendorff's test		
Saponins			
Tannins			

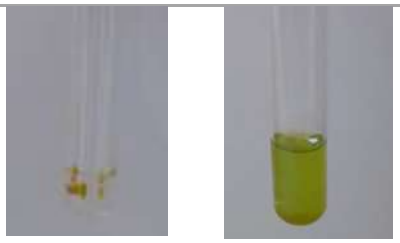
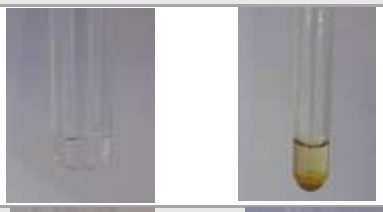
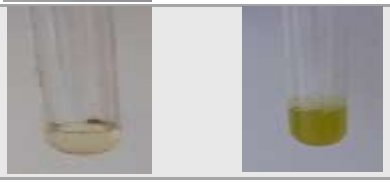
Sugars	
Anthraquinones	
Sterols	
Proteins	

Table 4: Overall results of the phytochemical screening of *n*-BuOHextract

Secondary metabolites *n*-BuOH extract	Observation	
	Before	After
Flavonoids		
Coumarins		

Alkaloids	Wanger's test	
	Dragendorff's test	
Saponins		
Tannins		
Sugars		
Anthraquinones		
Sterols		
Proteins		

Natural Resources for Human Health
eISSN: 2583-1194

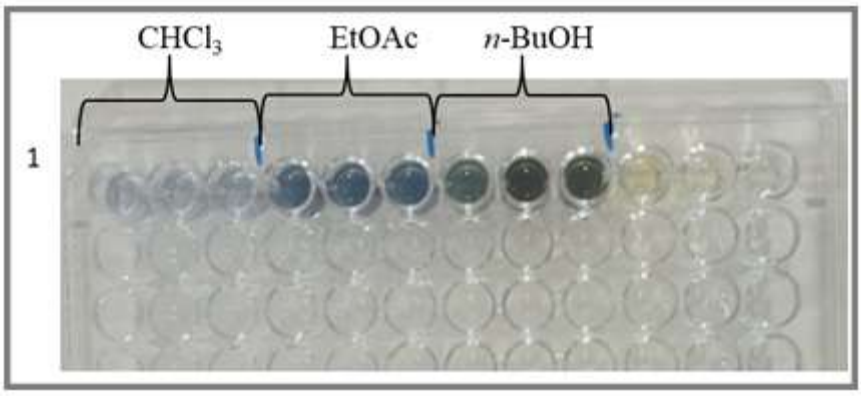


Figure 1: Polyphenol quantification plate for the three extracts: $CHCl_3$, AcOEt, and *n*-BuOH.

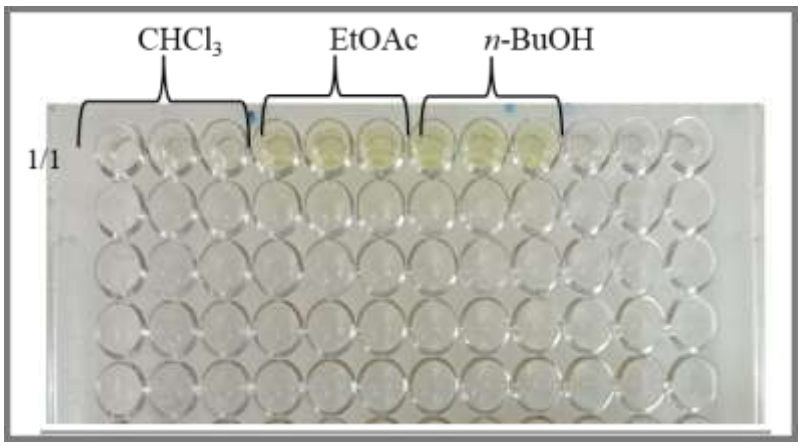


Figure 2: Flavonoid quantification plate for the three extracts: $CHCl_3$, AcOEt, and *n*-BuOH.

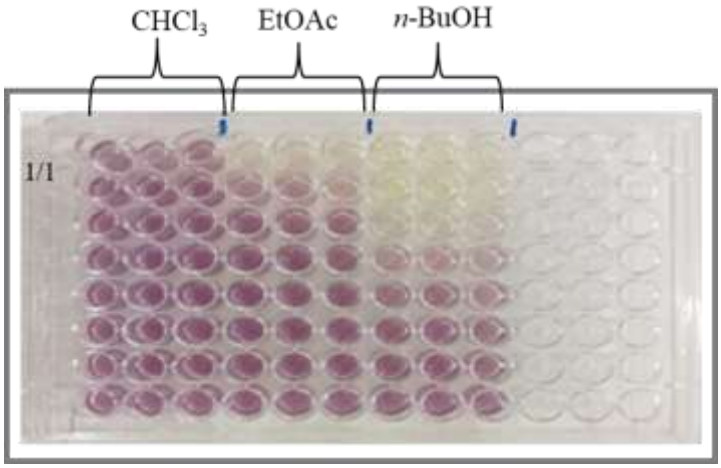


Figure 3: DPPH radical scavenging activity plate for the three extracts: $CHCl_3$, AcOEt, and *n*-BuOH.

Natural Resources for Human Health
eISSN: 2583-1194

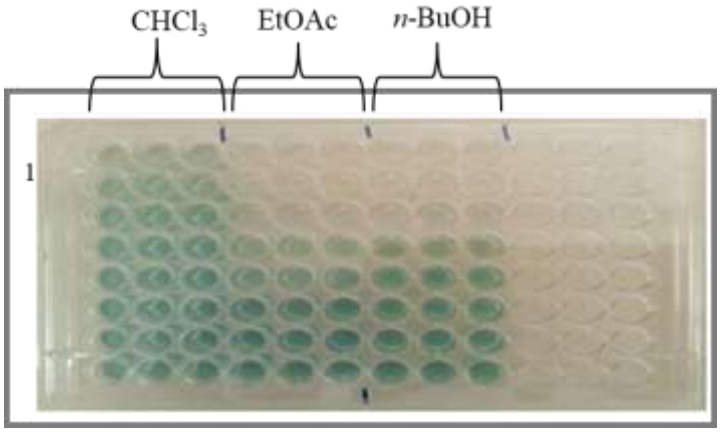


Figure 4: ABTS$^{\bullet+}$ radical cation scavenging activity plate for the three extracts: $CHCl_3$, AcOEt, and *n*-BuOH.

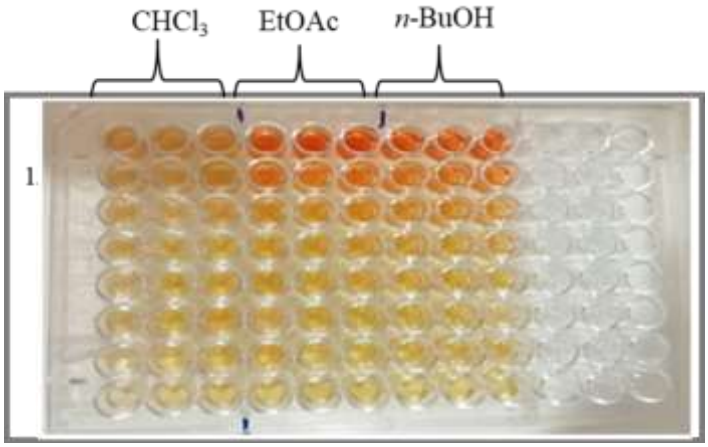


Figure 5: Phenanthroline assay plate for the three extracts: $CHCl_3$, AcOEt, and *n*-BuOH.